Metals and Materials International (2020) 26:1430–1440
https://doi.org/10.1007/s12540-019-00391-3

Development of Functionally Graded Tubes Based on Pure Al/Al_2O_3 Metal Matrix Composites Manufactured by Centrifugal Casting for Automotive Applications

Bassiouny I. Saleh[1,2] · **Mahmoud H. Ahmed**[1]

Received: 17 April 2019 / Accepted: 21 July 2019 / Published online: 29 July 2019

Abstract
This paper studies the influence of main parameters on the mechanical properties and wear behaviour of functionally graded materials pure Aluminum reinforced by various weight fractions of aluminium oxide (Al_2O_3). A Functionally graded (FG) pure aluminium/Al_2O_3 tube was processed by horizontal centrifugal casting method. The hollow tube dimensions are 230 mm outer diameter x 12 mm thickness x 180 mm length. The properties of these FG tubes were compared with unreinforced alloy. Hardness and tensile results in the radial direction showed that the hardness and tensile in accordance with the gradient microstructure was improved from inner zone to outer zone. Wear tests were carried out for different test duration at a constant sliding speed of 8 m/s and loads applied are 14, 24 and 40 N. In all test conditions the wear rate in the outer layer was minimum compared to other layers. In the surface analysis, scanning electron microscope indicated the presence of delamination, wear debris and cracks. FG tubes reinforced by Al_2O_3 particles have increased mechanical properties and wear resistance compared to its unreinforced alloy (matrix alloy) and is suitable for use in automobile and transport applications.

Keywords Wear · Functionally graded material (FGM) · Centrifugal casting · Metal matrix composites (MMC) · Pure aluminium · Aluminium oxide particles · Wear loss

1 Introduction

The demand for a variety of modern technological applications lies in engineering parts and structures that have location specific property requirements and performance under working conditions. A progressive transition to the properties motivates changes to the functions of a given location in order to meet the needs [1]. These tailored materials are functionally graded materials (FGMs). FGMs are relatively a new class of advanced heterogeneous composites where the composition and/or microstructure of the material is varied locally in order to regulate the physical and mechanical features of a component at a certain place. FGMs originated in 1984 first in Japan during the design of a space shuttle [2]. The phenomena of gradient structures, like bamboo, teeth, bone, wood, etc. and of certain conventional engineering materials are prevalent in nature [3].

Functionally graded materials (FGM) developments remain in its early stages and scope for developing a variety of real FGM for thermal protection systems for specific engineering applications such as automotive, aerospace, electronics, power generation, and bioengineering [4]. Because it has high temperature resistance, thermal characteristics, increased bonding and fracture toughness on the transition between metal matrix and reinforcement ceramic. The gradient transition zone in density, modulus of elasticity, grain size, or distribution of particles through an interface in the matrix of two or more materials can easily decrease thermal stresses, stress concentration, and design ability for various complex environments [5].

Most FGM study consists of multi-phase materials with the continuous changes in the properties leading to the formation of a controlled, non-uniform microstructure. The

✉ Bassiouny I. Saleh
bassiouny.saleh@hhu.edu.cn

[1] Production Engineering Department, Alexandria University, Alexandria 21544, Egypt

[2] College of Mechanics and Materials, Hohai University, Nanjing 211100, China

volume or weight fraction of enhanced particles or phases varies from one location to another in a component or structure. FGM processing is very much exigent and technologically relevant with its engineering components with gradient properties [6].

Among the different processing methods available to produce FGM [7], are the deposition of chemical or physical vapours, powder metallurgy [8, 9], centrifugal casting [10], centrifugal slurry casting, gravity settling [11], solid freeform Fabrication (SFF) including additive manufacturing [12], plasma spraying, laser deposition, physical vapour deposition [13], and infiltration, etc.

Centrifugal casting to produce FGMs is one of the easiest and most economical methods [14]. The components with axial symmetry generally process the cylindrical shapes using centrifugal force in the centrifugal casting method. When the FGM composite or melt containing different stages of the slurry undergoes a centrifugal force due to the difference of densities between matrix and reinforcement, different regions form during the melt with differentiated phase concentration; i.e. usually an outer zone and an inner zone with a transition zone between them [15, 16].

Many researchers focused on characterization of the mechanical, tribological and investigation of FGM microstructures prepared using completely different production techniques, matrix and reinforcing materials [17, 18]. In many examples of functionally graded materials prepared by centrifugal casting process hard reinforcements such as oxides or carbides or borides in the form of particles improve the mechanical properties and wear resistance of aluminium alloy [19].

For the past few years mechanical behaviour and wear resistance of centrifugally cast FGMs fabricated from Al-SiC or Al-Al_2O_3 particles had gained the interest of many researchers [20–23]. Experimental studies included the effects of the reinforcement particle percentage [17, 24], particle size [24], mould rotational speed [21, 25], the wear loads used and sliding speeds [25, 26] on mechanical properties and wear resistance [27].

Yılmaz and Buytoz [28] studied the effect of three different weight fractions (5, 10 and 15 wt%) of Al_2O_3 with average size 16 µm on mechanical and wear properties of FGM tube manufactured by vertical centrifugal casting method. Based on the results, the mechanical properties of FGM tube increased with the weight fraction of Al_2O_3 particles. Also, they found that greater wear resistance of composite was obtained with higher weight fraction (15 wt%) at the outer surface.

T. Prasad and T. Chikkanna [29] investigated the influence of weight fraction of particles on the microstructure, mechanical and fracture behaviour of FG 6061 Aluminium alloy/Al_2O_3 composite prepared by centrifugal casting. Four different weight fractions (5, 10, 15 and 20 wt%) and constant size (30–50 µm mean average size) of Al_2O_3 particles were used to produce FG composites. They reported that the FG composite improved the mechanical properties with enhanced fracture resistance compared to the base matrix alloy. Similar results were found in functionally graded AA6061 with 3, 5 and 10 wt% Al_2O_3 particles by Junus and Zulfia [30] they reported that the hardness of FGM pipes improves with the increasing in weight fraction of Al_2O_3 particles.

Radhika [19] investigated the effect of titanium disulphide (TiS_2) particles in LM 13 aluminium alloy. 10% weight fraction and average size 12 µm of titanium disulphide particles were used to produce FG composites manufactured by centrifugal casting technique. Microstructure of FGM tubes showed higher density reinforcement titanium disulphide at the outer surface due to higher concentration of TiS_2 particles. Also, the wear resistance of FGM tubes increased with decreasing applied load test.

Radhika and Vidyapeetham [31] fabricated and studied the effect of hybrid reinforcement type in of AlSi10 Mg alloy reinforced with ceramic particles (9 wt% Al_2O_3 + 3 wt% graphite) on wear behaviour. The centrifugal casting process was used to obtain FGM rings. The wear load was reported to be the most significant wear rate parameter, followed by sliding velocity and test duration.

Radhika and Raghu [32] discussed the effect of four different reinforcement types (B_4C, SiC, Al_2O_3 or TiB_2) in A319 alloy prepared by horizontal centrifugal casting route. Average particle size of 10 µm and 12 wt% of particles were used. They reported that the hardness at outer zone of FGM pipes improves in SiC particles compared to other particles, while tensile strength improves in SiC and TiB_2 particles.

Recently, Sam and Radhika [33] carried out the research work by fabricating functionally graded matrix composites through centrifugal casting route. The FG Cu alloy tube containing 10 wt% of alumina particles, of 10 µm particle size reinforcement was prepared to study the mechanical properties and wear behaviour. The Results show that, the addition of 10 wt% of Al_2O_3 particles to the copper alloy improves the mechanical and wear properties.

From the above literature survey, it's evident that only a few data are accessible on effect of Al_2O_3 particles and pure aluminium based mostly ceramic particles reinforced FGMs. To the most effective of our knowledge, no work is completed on composites using a matrix of pure Al with Al_2O_3 particles reinforcement. Hence, the primary goal of this work is to develop and fabricate functionally graded tubes created by horizontal centrifugal casting of pure Al–Al_2O_3 particles. Pure aluminium

Table 1 Chemical composition of commercially pure Al

Elements	Fe	Si	Cu	Zn	Ti	Mn	Mg	Al
wt%	0.015	0.015	0.004	0.001	0.002	0.001	0.001	99.97

Table 2 Typical composition of Al_2O_3 particles

Elements	Fe_2O_3	TiO_2	CaO	Other magnetic materials	Al_2O_3
wt%	0.7	1.7	1.1	0.2	96.3

is reinforced with various weight fractions of Al_2O_3 particles and different mould rotational speeds to prepare the FGM and compare the microstructure, mechanical and wear properties with unreinforced pure aluminium.

2 Experimental Procedures

2.1 Matrix and Reinforcement Materials

In this research, the studies were conducted using commercially pure aluminium (AA1010) as a matrix material (99.97%, Brinell Hardness 25 BHN and Ultimate Tensile Strength 80 MPa) to determine an appropriate procedure for producing centrifugal cast FG tubes within the tight pouring time available compare to Al alloys. In addition, the cost of the Al alloy is higher than that of pure aluminum, which introduces economic consideration in the cost of the FGM. The FG composite was reinforced with aluminum oxide particles (Al_2O_3) of average size of 16 µm Due to its high hardness and tribological resistance. The Al_2O_3 particles have density of 3690 kg/m^3 compared to commercially pure aluminium with density of 2700 kg/m^3. The alumina particles have terribly wear property and addition of aluminium oxide to pure aluminium matrix can increase the mechanical characterisation. Elemental composition of commercially pure aluminium and Al_2O_3 particles was determined through spectral analysis and is indicated in Tables 1 and 2.

2.2 Fabrication Process

Functionally graded tubes with 230 mm outer diameter and 12 mm thickness were manufactured by centrifugal casting process. Totally different average weight fractions of 2.5, 5 and 10 wt% Al_2O_3 particles were used. aluminium base metal melting was carried out in a graphite crucible at 725° C. Dried Al_2O_3 particle was added to the molten metal and stirred at a speed of 100 rpm for 5 min before pouring into the horizontal centrifugal casting feeder tube. The centrifugal casting machine was adapted its variable frequency inverter to provide completely different rotational speeds of 800, 900 and 1000 rpm. The centrifugal casting machine with details are shown in the previous publication [34]. Figure 1 shows the main steps of FGM tube production.

2.3 Microstructure Characterisation

In the present work, the gradient (distribution) of the Al_2O_3 particles produced across the thickness of the tube (12 mm) was investigated on separate surfaces of the FGM at distances from the outer zone of 1, 3, 6 and 9 mm. The specimens were cut from the FG tube then polished and etched with 0.5% diluted hydrofluoric acid (HF) for 15 s. Microstructural observation was performed using Zeiss Axiovert 25 CA compound optical microscope. On the worn surfaces of functionally graded tubes, the scanning microscope (SEM) was performed to check the mechanism of wear throughout wear testing and quality of distribution.

2.4 Mechanical Characterisation

The hardness evaluation and tensile behaviour were studied experimentally as detailed in the following sub-sections.

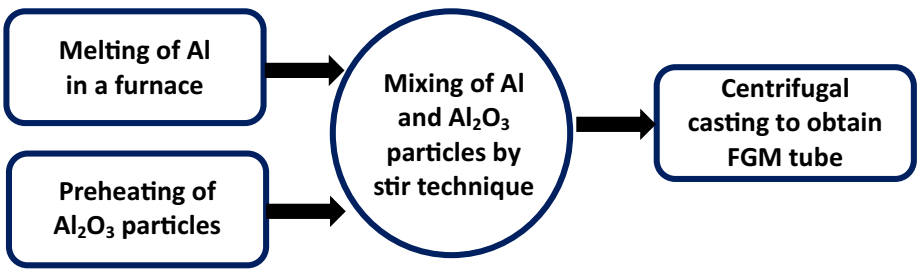

Fig. 1 Fabrication process flow chart

2.4.1 Tensile Strength Evaluation

The samples were cut on a milling machine and finished with fine emery paper. In the analysis of the effect of the distribution of Al_2O_3 particles over thickness, the tensile strength of the FGM tube was calculated using universal testing machine (UTM). The tensile testing was conducted on a tensile testing machine TUN-400, according to ISO 1608:1995 (mechanical testing of metals tensile testing of materials).

2.4.2 Hardness Evaluation

For measuring hardness of FGM tube, a Brinell hardness testing device was used for samples with a different weight fractions (2.5, 5 and 10 wt%) of Al_2O_3 particles. The MRB-250 was used as a hardness testing machine for a 62.5 N Load and a 5 mm steel ball indenter. The Brinell hardness values were calculated by the machine by capturing the dimensions of the indentation created by the steel ball indenter. The average of four surface hardness values was measured due to the hardness value of this specific surface. Likewise, the value of hardness was taken from outer surface of the FGM tube to inner surface within the thickness of FGM tube at completely different distances.

2.5 Wear Analysis

A pin-on-disk wear testing apparatus (TR-20, DUCOM) was used for acting dry sliding wear tests on four sets of samples taken from every FGM tube—manufactured with totally different weight fractions and mould rotational speed—so as to check the result of load and time throughout wear test. When the chill layer was removed by flat grinding, every set consisted of 3 specimens representing the most three zones (outer, middle, inner). Every sample was cut in sort of $20 \times 20 \times 35$ mm (axial × circumferential × radial) cuboid from the 12 mm thick cuboid. EN-31 stainless steel (63 HRC) is the rotating disk material. The wear tests were carried out at an average sliding speed of 8 m/s underneath four totally different traditional loads of 14, 24 and 44 N. On a 170 mm track of diameter at 900 rpm, the sample can rub against the rotating disk. Weight loss may be calculated by measuring the distinction in sample weight before and when the wear test to the closest milligram.

3 Results and Discussions

Microstructure characterisation, particle analysis, hardness measurement, tensile characteristics and wear evaluation are discussed in detail below.

3.1 Microstructure Characterisation

The microstructures reveal the existence of Al_2O_3 particles in the outer zone which ensures that segregation of the Al_2O_3 particles occurs under the action of the centrifugal force. When the molten FGM metal is poured into the mould, rapid cooling occurs at the interface between the molten metal and the mould and thus causing the outside tube to solidify without or restricting the movement of Al_2O_3 particles to the outer diameter. The surface is therefore taken into account for analysis at a distance of 1 mm from the outside diameter. Four different zones could be determined in each of the thickness of the sample according to the scheme described in Fig. 2: 1 mm, 3 mm, 6 mm and 9 mm from outer surface, respectively. The sample study shows that the graded Al_2O_3 particle distribution in the matrix begins at the highest concentration of Al_2O_3 particles 1 mm from the outer zone. Figure 2 shows the microstructure of specimens taken from different zones through the thickness of the produced FG tube. Figure 2a represents 1mm (the chill zone), Fig. 2b represents 3 mm (the outer zone), Fig. 2c represents 6 mm (the transition zone) and Fig. 2d represents the least concentration at 9 mm (the inner zone) thick from the outer surface. Figure 3 shows the panoramic view of the microstructures of pure Al–10 wt% Al_2O_3 particles FG tube from outer diameter to inner diameter along the radial direction. This panoramic perspective shows even lower magnification of the variations in the microstructure in various zones.

3.2 Particle Analysis

Image analysis technology has been used to analyse and calculate the distribution of Al_2O_3 particles across entirely different areas, from inner to outer FGM tube diameters, using the Image J software program. Automatic particle detection tools for contour borders are applied. The average concentration of Al_2O_3 particles in a one-millimetre-thick region is represented at all the information points shown in the figures. Figure 4 illustrates the concentration of Al_2O_3 particles through the various zones of the tube of FGM reinforced by 10 wt% of particles. The particles concentration of 800 rpm, 900 rpm and 1000 rpm are 37%, 39% and 43%, respectively, for the zone range of 0–1 mm (chill zone). In the next zone of the FG tube (1–2 mm), the average concentration of particles increased to 41%, 44% and 48%, respectively, at 800 rpm, 900 rpm and 1000 rpm. The decrease in the Al_2O_3 particles concentration rate is much higher in case of the 1000 rpm than the other two mould rotational speeds (800 rpm and 900 rpm). The gradient of the Al_2O_3 particles concentration can be estimated by the percentage of reduction in Al_2O_3 particles concentration per mm. For the 800 rpm,

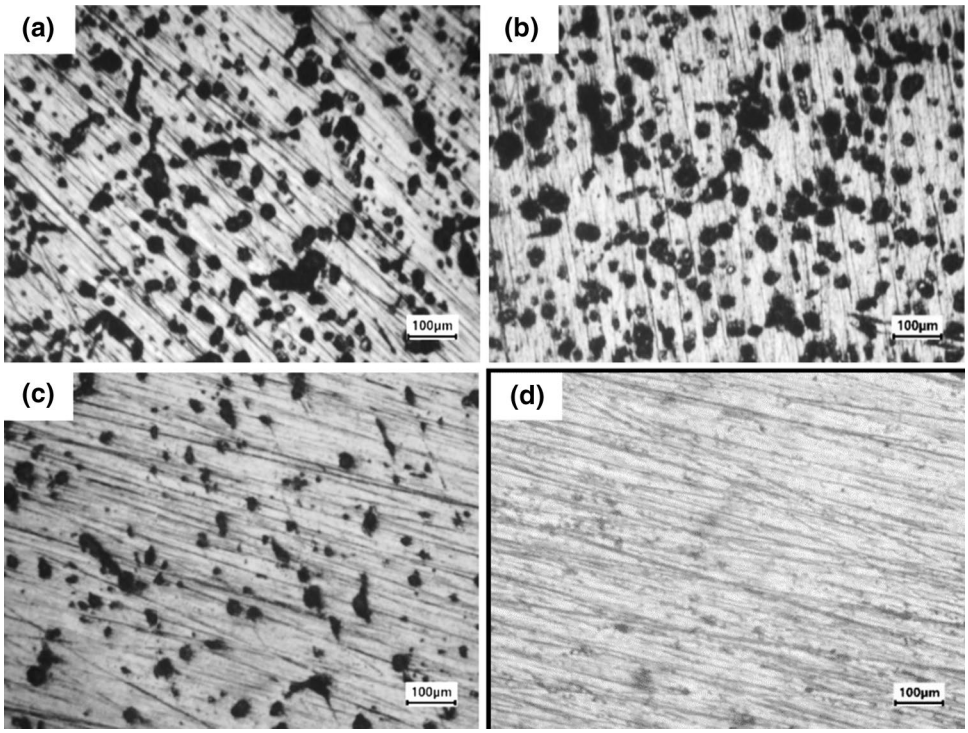

Fig. 2 Microstructure of FGM with 5 wt% Al_2O_3 particles at 900 rpm (**a** at 1 mm, **b** at 3 mm, **c** at 6 mm and **d** at 9 mm from outer surface of FG tube)

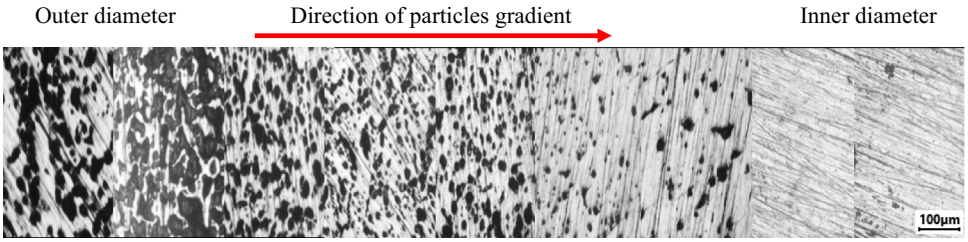

Fig. 3 Panoramic view of the microstructures of a pure Al–10 wt% Al_2O_3 FG tube along the radial direction at 1000 rpm

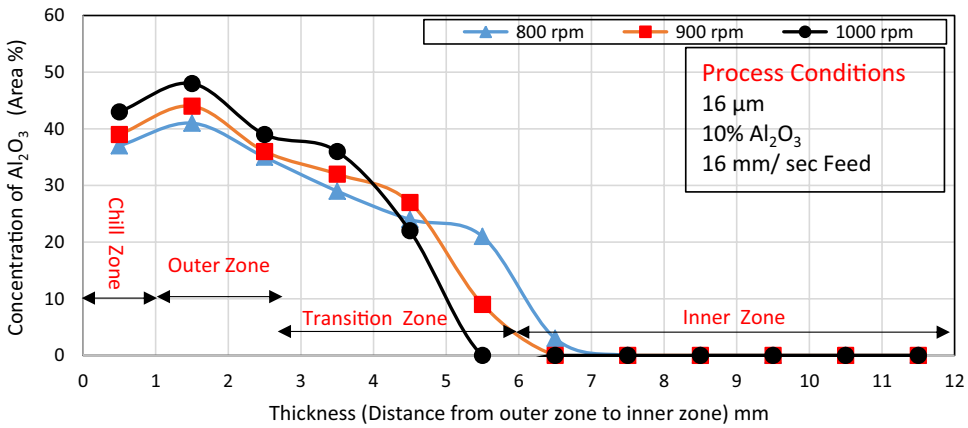

Fig. 4 Effect of mould rotational speed on concentration of Al_2O_3 particles

900 rpm and 1000 rpm mould rotational speeds, the gradients were calculated as 6%, 6.42% and 14% Al_2O_3 particles/mm, respectively.

The effect of weight fraction of Al_2O_3 particles on the distribution of the Al_2O_3 particles at the different zones along the distance from the outer zone to inner zone of

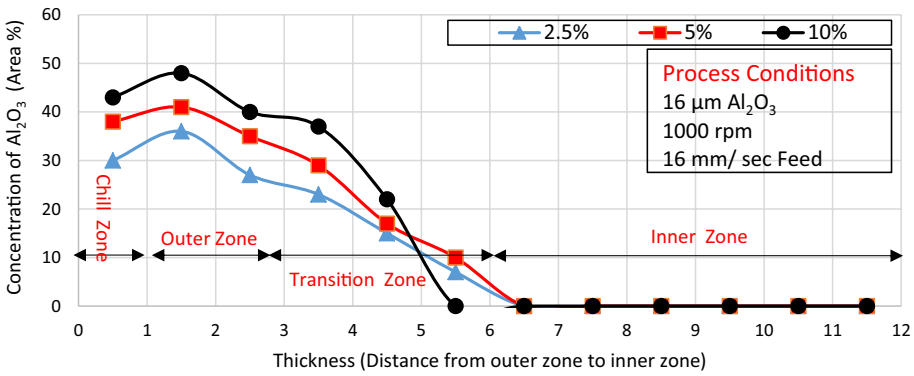

Fig. 5 Effect of weight fraction on concentration of Al_2O_3 particles

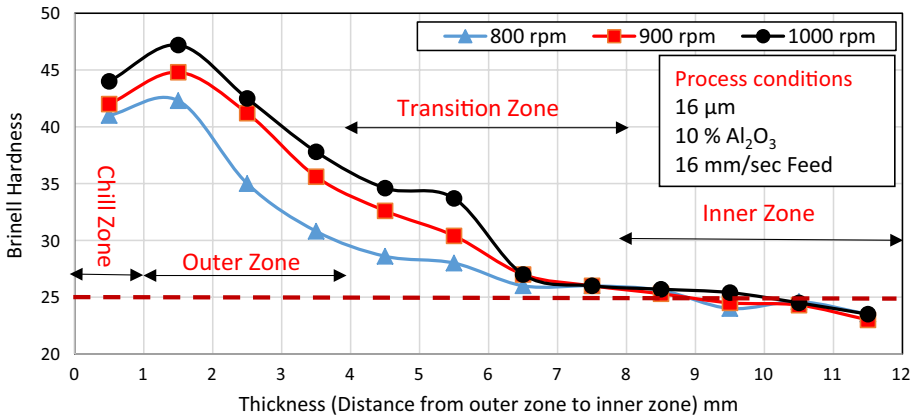

Fig. 6 Effect of rotational speed on brinell hardness

FG tube is illustrated in Fig. 5. As known, the centrifugal force is function of the particles mass and rotational speed. Thus, it is found that a 10 wt% of Al_2O_3 particles and the highest rotational speed (1000 rpm) will result in high concentration of Al_2O_3 particles at the outer surface. At smallest weight fraction of Al_2O_3 particles (2.5%) and highest rotational speed (1000 rpm) the concentration of Al_2O_3 particles at the outer zone will be less than the first case due to the reduction in centrifugal force. The distribution of the Al_2O_3 particles at different % of Al_2O_3 particles and mould rotational speeds are similar to the results obtained by [34, 35].

3.3 Hardness Measurement

The variation of Brinell hardness results of the FGM tubes with weight fraction of Al_2O_3 particles are shown in Fig. 6. From the figure, it is evident that the Brinell hardness value of the FG tube reinforced with particles is higher compared to unreinforced alloy (pure Al 25 BHN). At 1000 rpm and 10 wt% of particles, the highest Brinell hardness of 47.2 BHN is observed at 1.5 mm from the outer surface, and the inner zone at 11.5 mm is observed with a hardness value of 25 BHN. The Brinell hardness value of the FGM

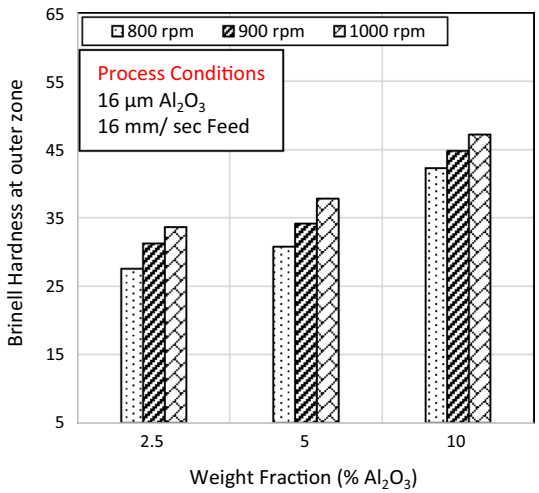

Fig. 7 Effect of mould rotational speed and % Al_2O_3 on brinell hardness at outer zone

tube decreases when the radial distance increases from the outer to inner surface. Results clearly show 45% and 27% improvement in Brinell hardness at outer and transition zone respectively compared with that of inner zone (pure aluminium). This improvement in Brinell hardness

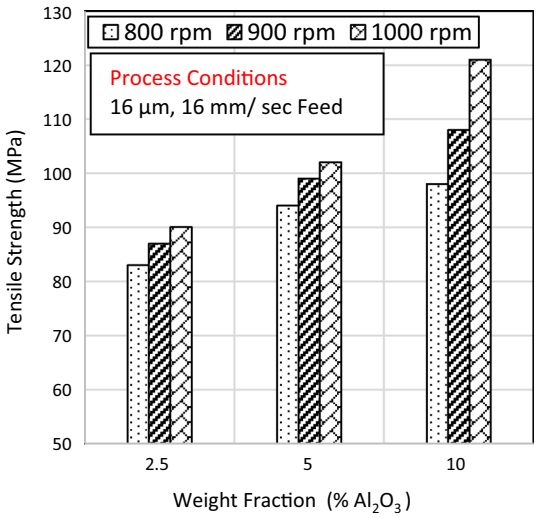

Fig. 8 Effect of Al_2O_3 particles weight fraction on ultimate tensile strength

is due to the presence of hard particles and their distribution (gradient) within the FGM tube, which depends on the centrifugal force.

The variations of hardness value at outer zone with different weight fraction of Al_2O_3 particles (average particle size 16 µm) for various rotational speeds (800 rpm, 900 rpm and 1000 rpm) as illustrated in Fig. 7. In general, with increasing the mould rotation speed, the Brinell hardness value increases. At any weight fraction, the FGM tube (Al–2.5 wt% Al_2O_3 particle, Al–5 wt% Al_2O_3 particle and Al–10 wt% Al_2O_3 particle) shows clearly higher hardness value than the as cast pure Al without particles for all mould rotational speed combinations. The high Brinell hardness value is mainly due to the enhancement of Al_2O_3 particle at the outer zone and the relatively clean, dense and defect-free surface created by the centrifugal force. According to Fig. 5 it is obvious that the highest weight fraction of Al_2O_3 particles the highest the hardness value at the same rotational speed and weight fraction. These results are consistent with earlier reports for the FGM Al-SiC_p alloy [15, 36].

3.4 Tensile Characteristics

The final tensile strength of the FGM tube against the weight fraction of Al_2O_3 particles at various mould rotating speeds is shown in Fig. 8. The addition of Al_2O_3 particles can seemingly improve the ultimate tensile strength of FGM composite. Minimum ultimate tensile strength (83 MPa) in the low mould rotational speed (800 rpm) with 2.5 wt% Al_2O_3 particles is observed primarily because of the low ceramic particle concentration which is much less resistant to deformation during testing. The presence of high Al_2O_3 concentration and enhanced compaction due to centrifugal force in the region towards the outer of the FGM tubes give increased strength. At 5 wt% Al_2O_3 particles of the FG tube centrifugal casting, the tensile strength value for low speed (800 rpm) and high speed (1000 rpm) are 94 MPa and 102 MPa, respectively. In case of FG tube with 10 wt% Al_2O_3 particles, has a tensile strength of 98 MPa in the low speed (800 rpm) and is raised to 98 MPa after the speed increased to 1000 rpm. Similar result is determined in another study [29].

3.5 Wear Evaluation

The results from wear tests for specimens in different weight fraction of Al_2O_3 particles from all zones and test durations will be discussed in this section. Half millimetre of each surface layer was removed to organize flat samples on internal and external sides.

3.5.1 Effect of Rotational Speed on Wear Loss of the Outer Zone

The rotational speed affects the centrifugal force and consequently affects the distribution of the Al_2O_3 particles furthermore because the hardness distribution and it's affecting the weight loss even it reaches 0.050 g at rotational speed 1000 rpm and 10% weight fraction. The variation of weight loss with completely different rotational speed and weight fraction of Al_2O_3 particles at 24 N load, 1 min duration and 8 m/s sliding velocity of FGM tube is shown within the Fig. 9. As mould rotational speed will

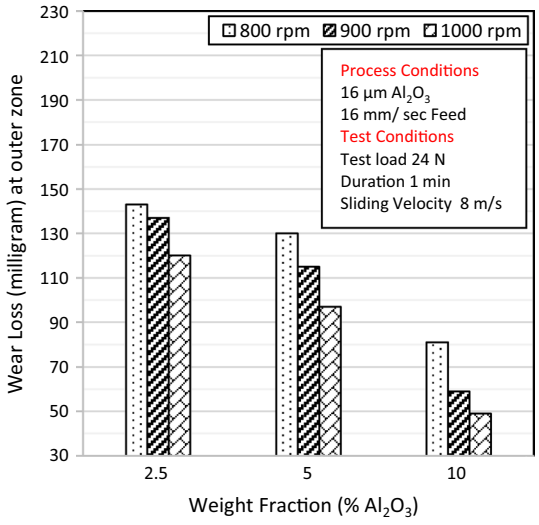

Fig. 9 Effect of mould rotational speed and weight fraction on weight loss of outer zone

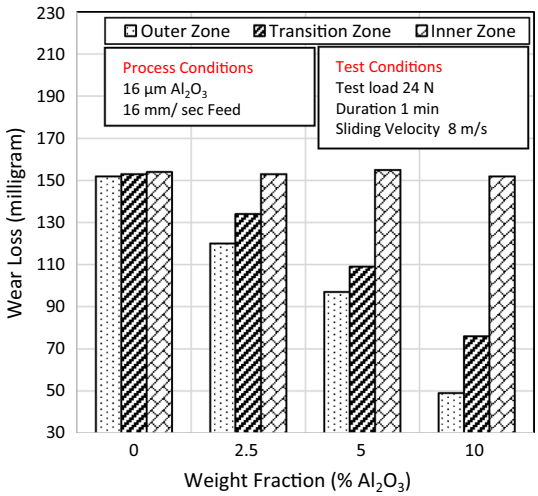

Fig. 10 Weight loss at different zones with increased Al_2O_3 weight fraction

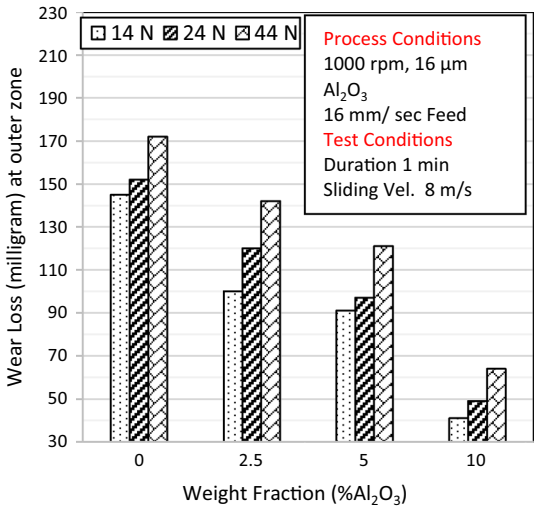

Fig. 11 Effect of applied load and wt% Al_2O_3 on weight loss of outer zone

increase, increase in wear loss is determined. Decreasing trend is observed with increase in quantity of wt% Al_2O_3 particles and mould rotational speed. For samples taken from outer zones of tubes with 10% weight fraction of Al_2O_3 particles, the lowest wear loss is observed irrespective of the used mould rotational speed. The results as indicated from Fig. 9 illustrates the declining trend of wear loss with increase in weight fraction percentage up to 10 wt% Al_2O_3 particles.

3.5.2 The Wear Loss at Different Zones

Figure 10 demonstrates the influence of the weight fraction on the wear loss. The weight fraction 10% shows the lowest wear rate and therefore the hardest outer zone. Moreover, because the enhanced wear rate is also due to a rise in the area of contact among the frictional heating surfaces which ends in a pin surface softening and the additional penetration of hard asperities in soft pin surface increased wear resistance. The results illustrate that the wear loss at outer zone for Al with 10 wt% Al_2O_3 particles FGM composite is simply 49 mg which represents only 65% of the wear loss of pure Al (154 mg).

3.5.3 Effect of Applied Load on Wear Loss of the Outer Zone

Figure 11 shows the variation of wear loss of FGM tube composites as an operate of varied loads and weight fraction of Al_2O_3 particles at 1 min period and sliding velocity 8 m/s. Figure 11 also shows that tube weight loss increases as test loads for all FGM composites and matrix material are increased. However, a decrease in wear loss is determined with increase in quantity of weight fraction of alumina (Al_2O_3) particles that helps to enhance the wear resistance and so decrease the wear loss. The pin surface at low applied load is mainly revealed as shown in Fig. 12, with fine and shallow grooves in the sliding direction. The weight loss will increase with increasing

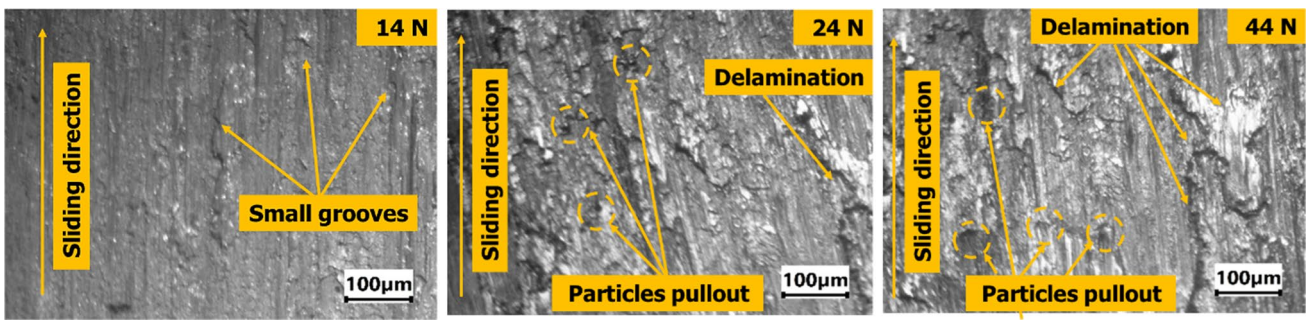

Fig. 12 Optical micrographs of wear surface for FGM (Al–5 wt% Al_2O_3) at different loads

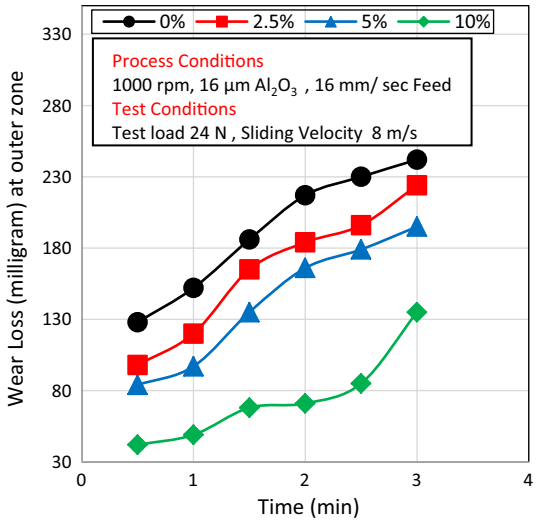

Fig. 13 Effect of weight fraction and duration on weight loss at outer zone

applied load because of increasing contacting pressure. The presence of hard alumina (Al_2O_3) particles will increase the wear resistance of the FGM tubes, particularly at outer and transition zones. The similar results of the applied load on the wear loss has also been reported in literature [15, 33].

3.5.4 Effect of Test Duration on Wear Loss of the Outer Zone

The cumulative weight loss of the outer zone of the FGM tube with test duration is shown in Fig. 13. The weight loss of the FGM tube at outer zone decreased with increasing the weight fraction of alumina (Al_2O_3) particles. Figure 14 shows the FGM tube macro examination which indicates a less weight loss and higher surface quality compared to matrix alloy. As shown earlier, the increased wear rate is due to the increasing area of the frictional heating between the connecting surfaces, which ends up in softening the surface of a pin and enlarged weight loss due to the penetration in soft pin surface by time of many hard asperities and similar result is determined in another study [34].

3.5.5 Scanning Electron Microscopy Analysis

Figure 15 shows the SEM for worn surfaces of the FGM tube with 10 wt% of Al_2O_3 at a sliding velocity of 8 m/s under constant load 24 N. The surfaces at distances 1 mm (chill zone Fig. 15a) and 3 mm (outer zone Fig. 15b) from outer surface show a minor number of cracks and grooves with less delamination due to presence of highest concentration of Al_2O_3 particles in these zones. As the distance to the inner zone increases, the wear mechanism from mild to severe wear changes. Figure 15c shows deep grooves with severe delamination at transition zone (6 mm from outer surface), due to the fact that there is relatively less concentration of Al_2O_3 particles. The contact between matrix and counter disk is high at distance 9 mm from outer zone (Fig. 15d) because there is a lot of scratching action and deep ploughing. Due to the reduced or no quantity of Al_2O_3 particles within the inner zone, the surface becomes ductile and form area without particles that increase the weight loss. Therefore, it is evident that, the outer zone of 3 mm with higher mechanical and wear properties makes the FGM tubes appropriate for the automotive applications like in engine cylinder liners, internal-combustion engine pistons and flywheels.

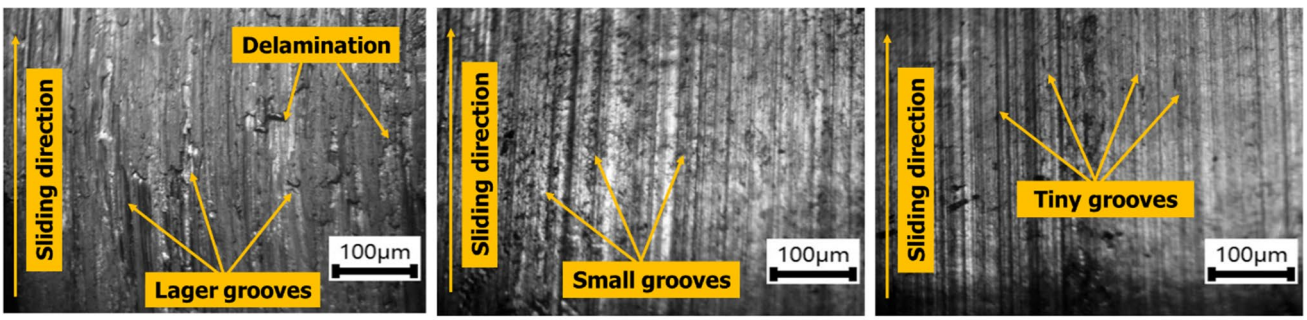

1000 rpm (0 wt% Al_2O_3 Particles) 1000 rpm (5 wt% Al_2O_3 Particles) 1000 rpm (10 wt% Al_2O_3 Particles)

Fig. 14 Examples of wear encountered in outer zone for different weight fractions

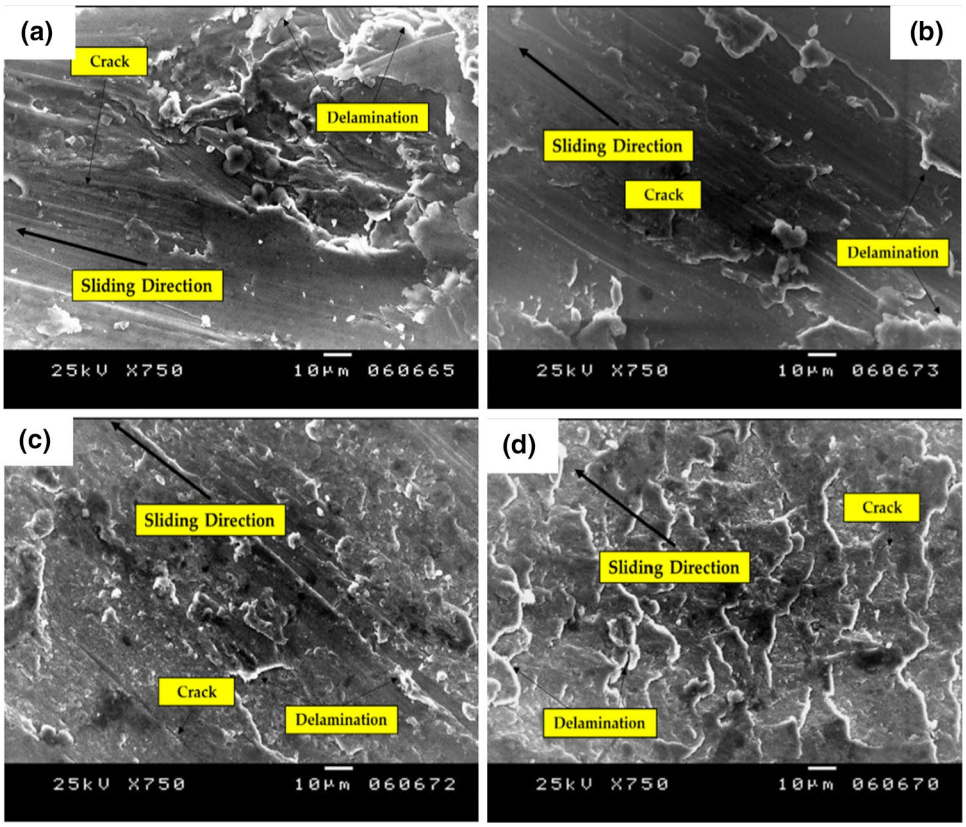

Fig. 15 SEM of wear encountered in different distances of FGM tube at 1000 rpm and 10% Al_2O_3 [**a** at 1 mm (chill zone), **b** at 3 mm (outer zone), **c** at 6 mm (transition zone) and **d** at 9 mm (inner zone) from outer surface of FG tube]

4 Conclusions

The major conclusions drawn from the present study on experimental investigations on microstructure, mechanical and wear behaviour of FG pure Al/Al_2O_3 are summarized.

1. The microstructures of the outer zone in all produced FG tubes reveal the presence of highest concentration of reinforcing particles. The highest filling volume has been achieved in case maximum rotational speed and highest weight fraction.
2. The thickness of the particle-rich zone in the FGM tubes decreases with the increase in the rotational speed. With the decrease of the rotating speed the maximum concentration of the Al_2O_3 particles at the outer zone decreases. However, this is associated with higher spread over the thickness of the degradation zone.
3. The presence of higher concentration of Al_2O_3 particles towards the outer zone leads to improve mechanical properties and wear resistance compared to the inner zone (matrix material). There are large differences in particle content between the outer zone and inner zone of all different cast FGMs tube processed at different processing speeds.
4. In all produced FG tubes, higher Brinell hardness is found in the outer zone than that in the concentration transition and inner zones. Increasing processing speed of mould increases the hardness at the outer region of FG tubes and reached maximum value at maximum processing speed.
5. The highest wear resistance is achieved in outer zones of all produced FG tubes, while lower resistance could be measured in the concentration transition and inner zones.
6. These FGM tubes can be successfully used for manufacturing high specific strength components with very high surface hardness and wear resistances in automotive and transport applications.

Acknowledgements The authors would like to thank the Production Engineering Department of Alexandria University and the technicians in appreciation for the help they offered. The authors wish to thank the faculty management for their financial support. Special thanks to LORD INTERNATIONAL Co. for your assistance and participation in this project.

Compliance with Ethical Standards

Conflict of interest The authors declare that they have no conflict of interest.

References

1. E. Akinlabi, R. Mahamood, *Functionally Graded Materials* (Springer, Cham, 2017)
2. M. Gasik, Int. J. Mater. Prod. Technol. **39**, 20 (2010)
3. A.k. Ashwinkumar, Int. Res. J. Eng. Technol.**4**, 890 (2017)
4. H. Sai, A review on functionally gradient materials (FGMs) and their applications, Int. J. Curr. Eng. Tech. **8**, 79 (2018)
5. M. Naebe, K. Shirvanimoghaddam, Appl. Mater. Today **5**, 223 (2016)
6. R.S. Parihar, S.G. Setti, R.K. Sahu, Sci. Eng. Compos. Mater. (2016). https://doi.org/10.1515/secm-2015-0395
7. B. Kieback, A. Neubrand, H. Riedel, Mater. Sci. Eng. A **362**, 81 (2003)
8. R. Kumar, C. Chandrappa, Int. J. Innov. Res. Sci. Eng. Technol. **3**, 15464 (2014)
9. F. Erdemir, A. Canakci, T. Varol, Trans. Nonferrous Met. Soc. China **25**, 3569 (2015)
10. T.P.D. Rajan, R.M. Pillai, B.C. Pai, Mater. Charact. **61**, 923 (2010)
11. Y. Watanabe, H. Sato, Nanocomposites with unique properties and applications in medicine and industry, Review fabrication of functionally graded materials under a centrifugal force (InTech, China, 2011), pp. 133–150
12. D.W. Hutmacher, M. Sittinger, M.V. Risbud, Trends Biotechnol. **22**, 354 (2004)
13. V. Bhavar et al., A review on functionally gradient materials (FGMs) and their applications, Mat. Sci. Eng. **229**, 12 (2017)
14. B. Saleh, J. Jiang, A. Ma, D. Song, D. Yang, Met. Mater. Int. (2019). https://doi.org/10.1007/s12540-019-00273-8
15. E. Jayakumar, A.P. Praveen, T.P.D. Rajan, B.C. Pai, Trans. Indian Inst. Met. (2018). https://doi.org/10.1007/s12666-018-1442-5
16. N. Radhika, Trans. Indian Inst. Met. **70**, 145 (2016)
17. A.S. Karun, T.P.D. Rajan, U.T.S. Pillai, B.C. Pai, J. Compos. Mater. (2015). https://doi.org/10.1177/0021998315602946
18. E. Jayakumar, J.C. Jacob, T.P.D. Rajan, M.A. Joseph, B.C. Pai, Metall. Mater. Trans. A **47**, 4306 (2016)
19. N. Radhika, Tribol. Ind. **38**, 425 (2016)
20. A. Velhinho, J.D. Botas, E. Ariza, J.R. Gomes, L.A. Rocha, Mater. Sci. Forum **456**, 871 (2004)
21. A.C. Vieira, P.D. Sequeira, J.R. Gomes, L.A. Rocha, Wear **267**, 585 (2009)
22. G. Zheng, et al, Met. Mater. Int. (2019). https://doi.org/10.1007/s12540-019-00357-5
23. K.V. Babu, J.T.W. Jappes, T.P.D. Rajan, J. Mater. Des. Appl. **230**, 182 (2014)
24. T.R. Prabhu, Arch. Civ. Mech. Eng. **17**, 20 (2016)
25. N. Radhika, R. Raghu, Trans. Indian Inst. Met. (2017). https://doi.org/10.1007/s12666-017-1204-9
26. M. Ravikumar, H. Reddappa, R. Suresh, Silicon. (2018). https://doi.org/10.1007/s12633-018-9788-1
27. I.M. EL-Galy, B.I. Bassiouny, M.H. Ahmed, Key Eng. Mater. **786**, 276 (2018)
28. S.O. Yılmaz, S. Buytoz, J. Mater. Sci. **42**, 4485 (2007)
29. T. Prasad, T. Chikkanna, Int. J. Adv. Eng. Technol. **II**, 161 (2011)
30. S. Junus, A. Zulfia, Mater. Sci. Forum **857**, 179 (2016)
31. A. Vidyapeetham, N. Radhika, Tribol. Ind. **36**, 188 (2014)
32. N. Radhika, R. Raghu, Trans. Nonferrous Met. Soc. **26**, 905 (2016)
33. M. Sam, N. Radhika, Part. Sci. Technol. **37**, 220 (2019)
34. I.M. El-Galy, M.H. Ahmed, B.I. Bassiouny, Alex. Eng. J. **56**, 371 (2017)
35. T.P.D. Rajan, R.M. Pillai, B.C. Pai, Int. J. Cast Met. Res. **21**, 214 (2008)
36. T.P.D. Rajan, B.C. Pai, Mater. Sci. Forum **690**, 157 (2011)